

INTERMETALLIC AND ELECTRICAL INSULATOR COATINGS  
ON HIGH-TEMPERATURE ALLOYS IN LIQUID-LITHIUM ENVIRONMENTS\*

J.-H. Park  
Energy Technology Division  
Argonne National Laboratory  
Argonne, Illinois 60439

June 1994

The submitted manuscript has been authored by a contractor of the U. S. Government under contract No. W-31-109-ENG-38. Accordingly, the U. S. Government retains a nonexclusive, royalty-free license to publish or reproduce the published form of this contribution, or allow others to do so, for U. S. Government purposes.

**DISCLAIMER**

This report was prepared as an account of work sponsored by an agency of the United States Government. Neither the United States Government nor any agency thereof, nor any of their employees, makes any warranty, express or implied, or assumes any legal liability or responsibility for the accuracy, completeness, or usefulness of any information, apparatus, product, or process disclosed, or represents that its use would not infringe privately owned rights. Reference herein to any specific commercial product, process, or service by trade name, trademark, manufacturer, or otherwise does not necessarily constitute or imply its endorsement, recommendation, or favoring by the United States Government or any agency thereof. The views and opinions of authors expressed herein do not necessarily state or reflect those of the United States Government or any agency thereof.

Manuscript submitted for publication in Proceedings of a Symposium on High-Temperature Coatings-I at the TMS Fall Meeting, October 2-6, 1994, Rosemont, IL

\*This work has been supported by the U.S. Department of Energy, Office of Fusion Energy Research under Contract W-31-109-Eng-38.

**MASTER** *da*

DISTRIBUTION OF THIS DOCUMENT IS UNLIMITED

## **DISCLAIMER**

**Portions of this document may be illegible in electronic image products. Images are produced from the best available original document.**

# INTERMETALLIC AND ELECTRICAL INSULATOR COATINGS ON HIGH-TEMPERATURE ALLOYS IN LIQUID-LITHIUM ENVIRONMENTS\*

J.-H. Park

Energy Technology Division  
Argonne National Laboratory  
Argonne, Illinois 60439

## Abstract

In the design of liquid-metal cooling systems for fusion-reactor blanket applications, the corrosion resistance of structural materials and the magnetohydrodynamic (MHD) force and its subsequent influence on thermal hydraulics and corrosion are major concerns. When the system is cooled by liquid metals, insulator coatings are required on piping surfaces in contact with the coolant. The objective of this study is to develop stable corrosion-resistant electrical insulator coatings at the liquid-metal/structural-material interface, with emphasis on electrically insulating coatings that prevent adverse MHD-generated currents from passing through the structural wall, and Be-V intermetallic coatings for first-wall components that face the plasma. Vanadium and V-base alloys (V-Ti or V-Ti-Cr) are leading candidate materials for structural applications in a fusion reactor. Various intermetallic films were produced on V-alloys and on Types 304 and 316 stainless steel. The intermetallic layers were developed by exposure of the materials to liquid Li containing <5 at.% dissolved metallic solutes (e.g., Al, Be, Si, Pt, and Cr) at temperatures of 416-880°C. In principle, intermetallic layers can be converted to electrically insulating coatings by in-situ oxidation or nitration. Oxygen or oxygen/nitrogen-rich surface layers were developed on V-base alloys by exposure to flowing 99.999%-pure Ar or N<sub>2</sub> at temperatures of 500-1030°C. CaO electrical insulator coatings were produced by reaction of the oxygen-rich layer with <5 at.% Ca dissolved in liquid Li at 400-700°C. The reaction converted the oxygen-rich layer to an electrically insulating film. This coating method is applicable to reactor components because the liquid metal can be used over and over; only the solute within the liquid metal is consumed. The technique can be applied to various shapes (e.g., inside/outside of tubes, complex geometrical shapes) because the coating is formed by liquid-phase reaction. This paper will discuss initial results on the nature of the coatings (composition, thickness, adhesion, surface coverage) and their in-situ electrical resistivity characteristics in liquid Li at high temperatures.

---

\*Work supported by the U.S. Department of Energy, Office of Fusion Energy Research under Contract W-31-109-Eng-38.

## 1. Introduction

Corrosion resistance of structural materials and magnetohydrodynamic (MHD) force and its influence on thermal hydraulics are major concerns in the design of liquid-metal cooling systems for fusion first-wall/blanket applications [1-3]. The objective of this study is to develop in-situ stable corrosion-resistant coatings, as well as insulator coatings at the liquid-metal/structural-material interface. The electrically insulating coatings should be capable of forming on various shapes such as the inside of tubes or irregular shapes during operational conditions to prevent adverse currents that are generated by MHD forces from passing through the structural wall in the fusion reactor, shown schematically in Fig. 1. [4] The coatings could also improve general corrosion resistance and act as a diffusion barrier for hydrogen isotopes, viz., deuterium and tritium.

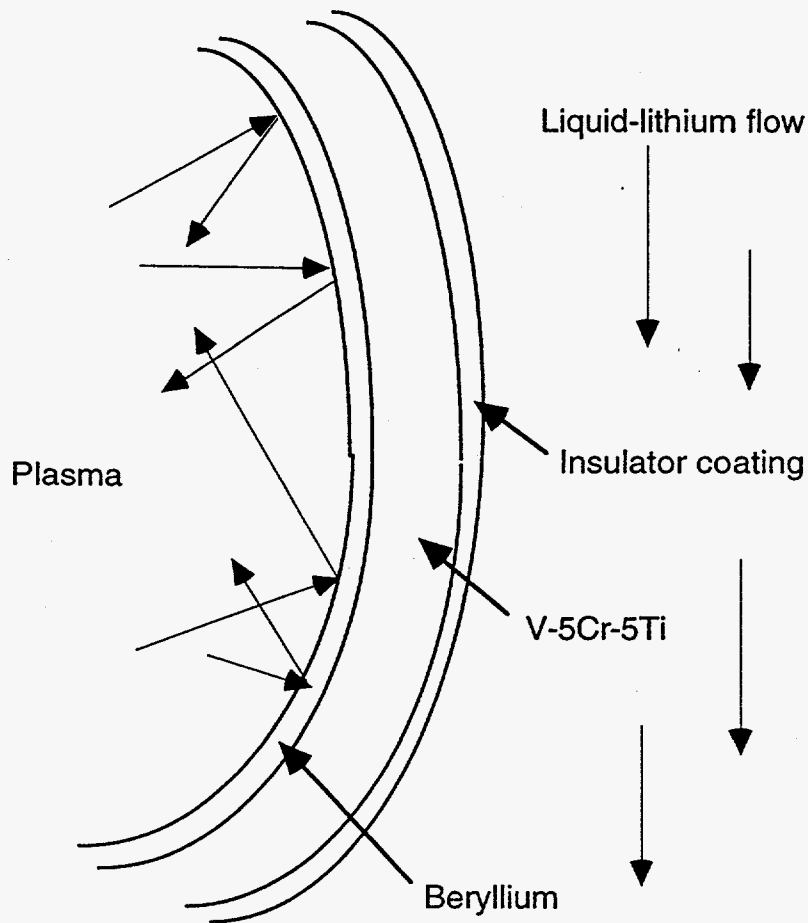


Figure 1. Schematic drawing of the first wall in a fusion reactor

In this study, in-situ coatings in liquid-Li were selected based on screening test results of the compatibility of ceramic materials in liquid-Li. Even though we examined ceramic materials that were thermodynamically stable in liquid Li, most of the ceramic materials dissolved. We conclude that this was caused by thermodynamically unstable impurities that formed at grain boundaries during the fabrication process, e.g., O in AlN. For example, sintered AlN disintegrated in liquid Li, but AlN exhibited compatibility when yttrium, which acts as an oxygen getter and stabilized the material (Y/Y<sub>2</sub>O<sub>3</sub>), was added during sintering. [5] Three types of experiments have been conducted to develop electrical insulator coatings for use in liquid Li: (a) a screening test for the candidate ceramic materials in liquid Li [5,6], (b) in-situ fabrication of intermetallic layers *for subsequent conversion to electrically insulating layers by oxidation or nitration*, (c) reaction of an oxygen-rich surface layer in a V-base alloy with Ca dissolved in liquid Li to produce a ceramic insulator coating (CaO) on the material, and (d) in-situ electrical resistance measurements of insulator coatings on V-alloys as a function of time and temperature in Li.

## **2. Formation of intermetallic coatings on high-temperature alloys in liquid Li**

Various intermetallic layers were developed by exposure of V-5Cr-5Ti and Types of 304 and 316 stainless steel to liquid Li containing dissolved metallic solutes (Al, Be, Mg, Si, Ca, Pt, Y, and Cr), where most of the solutes were chosen based on thermodynamic stability of their metal oxides or nitrides in Li as well as results of compatibility screening tests for ceramic materials in Li.

### *2.1. Aluminide coatings*

Aluminide coatings that form on structural alloys during exposure to liquid Li that contained dissolved Al suggest a means for producing stable electrical insulator layers, such as AlN, by subsequent nitration of the intermetallic layer in the liquid-metal environment [5]. The formation of several aluminides (V<sub>x</sub>Al<sub>y</sub>) that contain >40–50 at.% Al on V-base alloys can be predicted from the V-Al phase diagram [7,8]. The Al-Li phase diagram indicates that Al is soluble in liquid Li, whereas V is not soluble in Li [8]. These phase relations make up the underlying basis for the formation of aluminide coatings on V and its alloys in liquid Li. Aluminide coatings were produced on the alloys by exposure to liquid Li that contained 3–5 at.% Al in sealed V and V-20Ti capsules. The nature of aluminide coatings formed on V, Ti, and V-5Ti, and V-20Ti, V-5Cr-5Ti and V-15Cr-5Ti and Types 304 and 316 stainless steel at 650–880°C was investigated.

The specimens and liquid Li were contained in V-20Ti and V or stainless steel capsules that were placed in a larger stainless steel container. An Ar cover gas (99.999% pure) was maintained in the system to prevent oxidation of the V capsules and the Li. The whole

assembly was placed in a vertical furnace. At the end of the test, the capsules were cut open above the Li level to remove the samples. The capsules were placed in a beaker of water to dissolve the small volume of Li, and the samples were removed and cleaned ultrasonically in acetone and ethanol and dried in air. The samples were examined by optical microscopy and scanning-electron microscopy (SEM), and analyzed by EDS and X-ray diffraction. Hardness of the coating layers and bulk alloys was determined by Vickers indentation measurements with a Leitz microhardness tester. Degree of surface coverage and thickness of the layers varied considerably, depending on exposure time and temperature. At temperatures and exposure times of  $<800^{\circ}\text{C}$  and  $<90$  h, respectively, the aluminide layers were not uniform. At the lowest temperature ( $775^{\circ}\text{C}$ ), small grains on the surface began to connect with neighboring grains by a grain-growth mechanism. At the highest temperature ( $880^{\circ}\text{C}$ ), the microstructure reveals that grain size is larger by at least one order of magnitude. Dependence of Al concentration at the coating surface on temperature is shown for several samples in Fig. 2. The EDS analysis of the coating surface was obtained over a region of  $1,000 \times 1,000 \mu\text{m}$ .

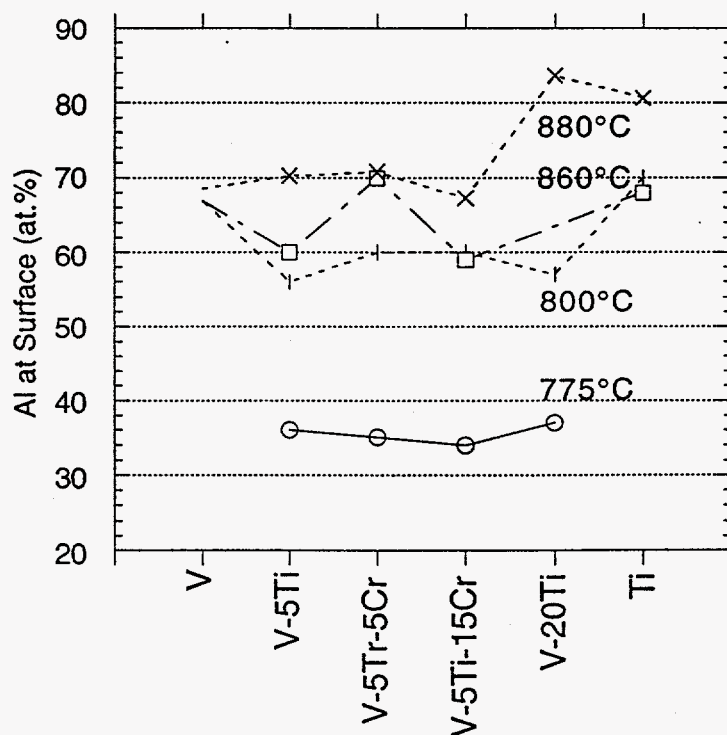


Figure 2. Aluminum content of aluminized surfaces formed on several V-base alloys and Ti at several temperatures from  $775$  to  $880^{\circ}\text{C}$

A typical cross section of an aluminide coating layer is virtually defect-free, but an array of small defects is present beneath the compact layer. These defects may be clustered near a dislocation zone that is depleted in Al and rich in Li because of fast diffusion of Li via dislocations. Composition-vs.-depth profiles for the V and V-20Ti specimens are shown in Fig. 3. The depth of Al interdiffusion in V-20Ti is three to four times greater than in pure V at 860°C, which suggests a higher mobility of Al in V-20Ti than in V. Vickers hardness measurements of the aluminide layers and the underlying V and V-20Ti alloy were conducted at 25- and 50-g loads. The aluminide layers were harder than either V or V-20Ti, which can be attributed to interstitial Al atoms in the cubic lattice of V. Because the distribution of nonmetallic elements (O, N, C, H) between V-base alloys and Li favors the Li, the alloys tend to become depleted in these constituents during exposure to high-temperature Li. Consequently, the hardness increase is most likely caused by diffusion of Al, C, and N into V and V-20Ti. Our experience indicates that V becomes more ductile after exposure to liquid Li in a closed capsule. The aluminide coating is not only present on the surface of the tube and the face of the disk, but also penetrates the 1-mm space between the V-20Ti tube and V disk. The thickness of the coating in this region is similar to that on the inner surface of the tube and the disk exposed to liquid Li. The coating behavior suggests that bulk diffusion is the main process. Similarly, an iron aluminide coating was produced on Types of 304 and 316 stainless steel. Microstructures of surface and cross section are shown in Fig. 4.

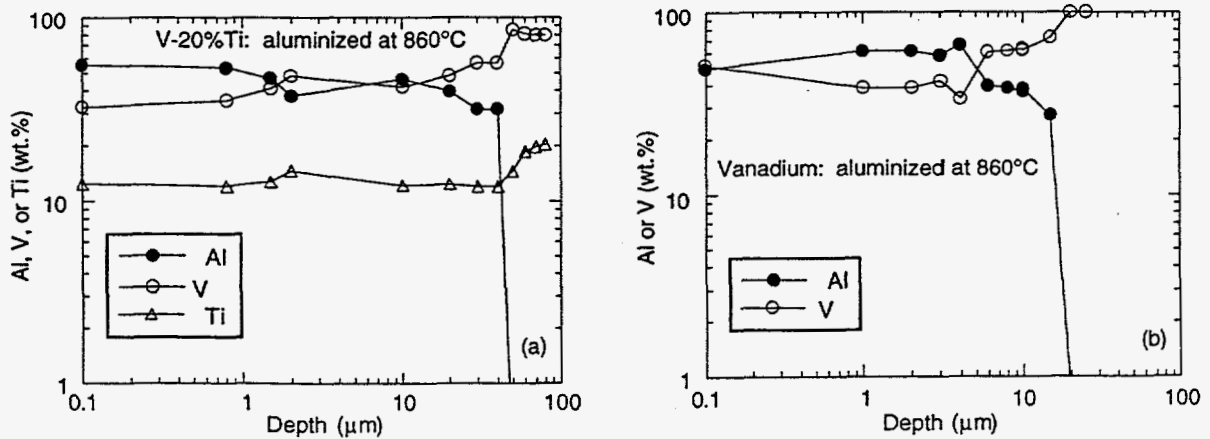


Fig. 3. Chemical composition as a function of depth for aluminide layers on (a) V-20Ti and (b) V

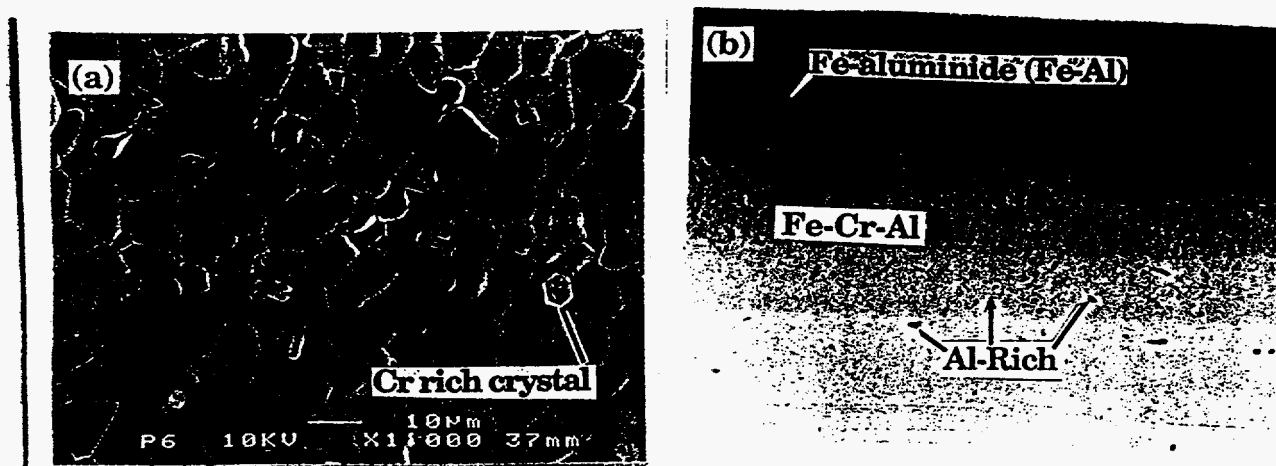


Fig. 4. Typical aluminide surface formed on Types 304 <sup>or</sup> and 316 stainless steel at 650°C  
(a) Surface and (b) cross section

## 2.2. Be coating on V-5Cr-5Ti

Beryllium forms intermetallic phases with many elements, namely, Ba, C, Ca, Co, Cr, Cu, Fe, Hf, Ir, Mg, Mn, Mo, N, Nb, Ni, O, Po, Pt, Pu, Re, Rh, Ru, Sb, Sc, Se, Sr, Ta, Th, Ti, U, V, W, Y, Yb, and Zr. Consequently, this property can be potentially useful in the formation of Be-(V, Cr, Ti) intermetallic coatings on V-Cr-Ti alloys. Beryllium intermetallic coatings that form on structural alloys during exposure to liquid Li that contains dissolved Be suggest a means for producing stable electrical insulator layers, such as BeO, Be<sub>3</sub>N<sub>2</sub>, or Be-O-N, by subsequent oxidation or nitration of the intermetallic layer in the liquid-metal environment. According to the Be-V binary phase diagram shown in Fig. 5, Be<sub>12</sub>V and Be<sub>2</sub>V intermetallic phases are present. Similarly, Cr and Ti form CrBe<sub>2</sub> and CrBe<sub>12</sub> and TiBe<sub>2</sub>, TiBe<sub>3</sub>, Ti<sub>2</sub>Be<sub>12</sub>, and TiBe<sub>17</sub>, respectively. Thus, the major alloy constituents of V-5Cr-5Ti can form intermetallic phases with Be. Intermetallic phases can also form when Fe-Cr-based alloys are exposed to liquid Li that contains dissolved Be. Figure 6 shows the Be<sub>2</sub>V intermetallic phase on the surface of a V-5Cr-5Ti specimen, after exposure to liquid Li containing Be, and a Be depth profile obtained by secondary-ion mass spectroscopy.

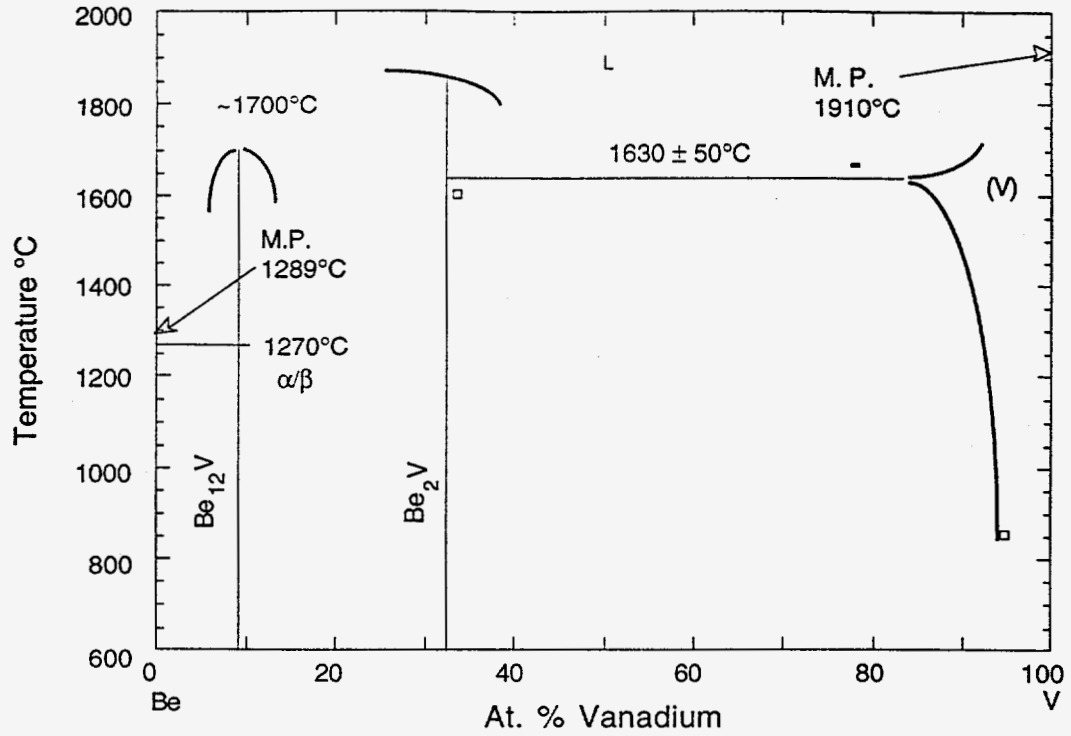


Fig. 5. Be-V phase diagram

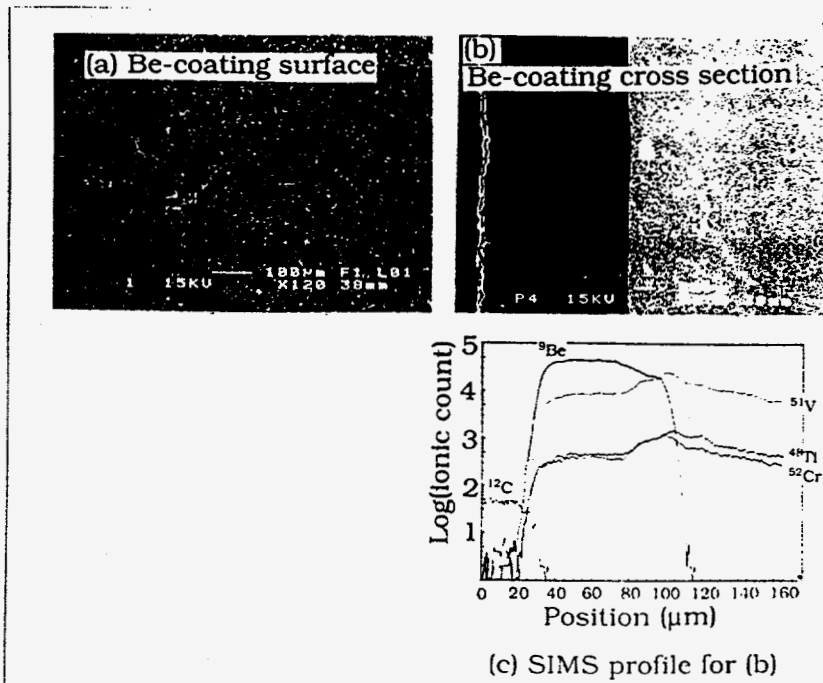


Fig. 6. (a, b)  $\text{Be}_2\text{V}$  intermetallic phase on a V-5Cr-5Ti surface and cross section, and (c) Be depth profile obtained by secondary-ion mass spectroscopy

### 2.3. Silicide coating on V-5Cr-5Ti

Similar to the formation of aluminide or beryllide on V-alloys, the kinetics of silicide growth on the V-5Cr-5Ti at 760°C and 890°C are shown in Fig. 7. Figure 8 shows a typical SEM photograph and EDS profile of the surface of a silicide layer that formed in liquid Li containing 3-4 at.% silicon at 890°C for 30 h. According to the results of X-ray diffraction, the silicide layer was composed of  $V_3Si$  and  $V_5Si_3$ . Silicide coatings formed on Types 316 and 304 stainless steels at lower temperatures than those on V-5Cr-5Ti. The surface of a silicide coating on Type 316 stainless steel that formed at 650°C is shown in Fig. 8.

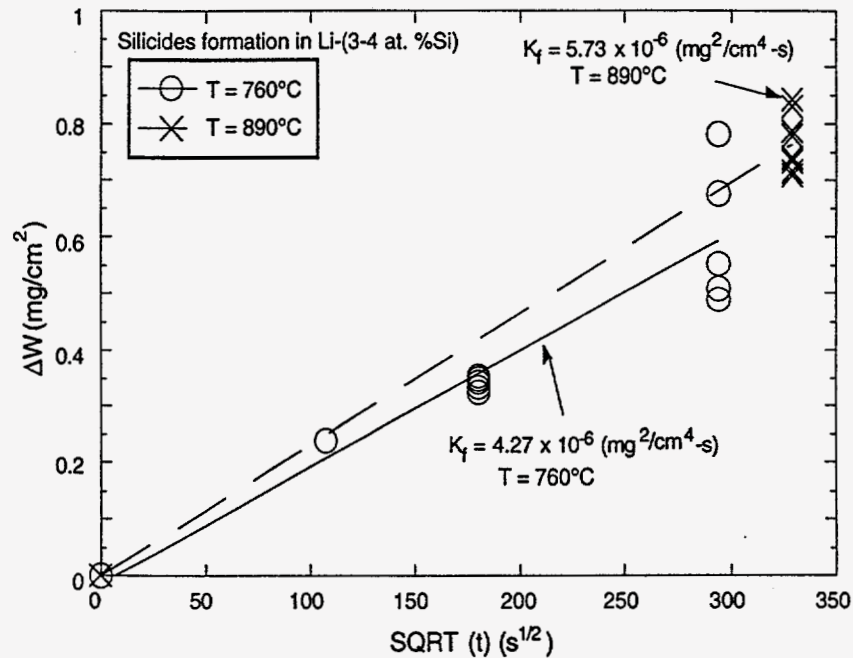


Fig. 7. Weight change vs. square root time for silicide coatings on V-5Cr-5Ti in liquid Li at 760°C and 890°C

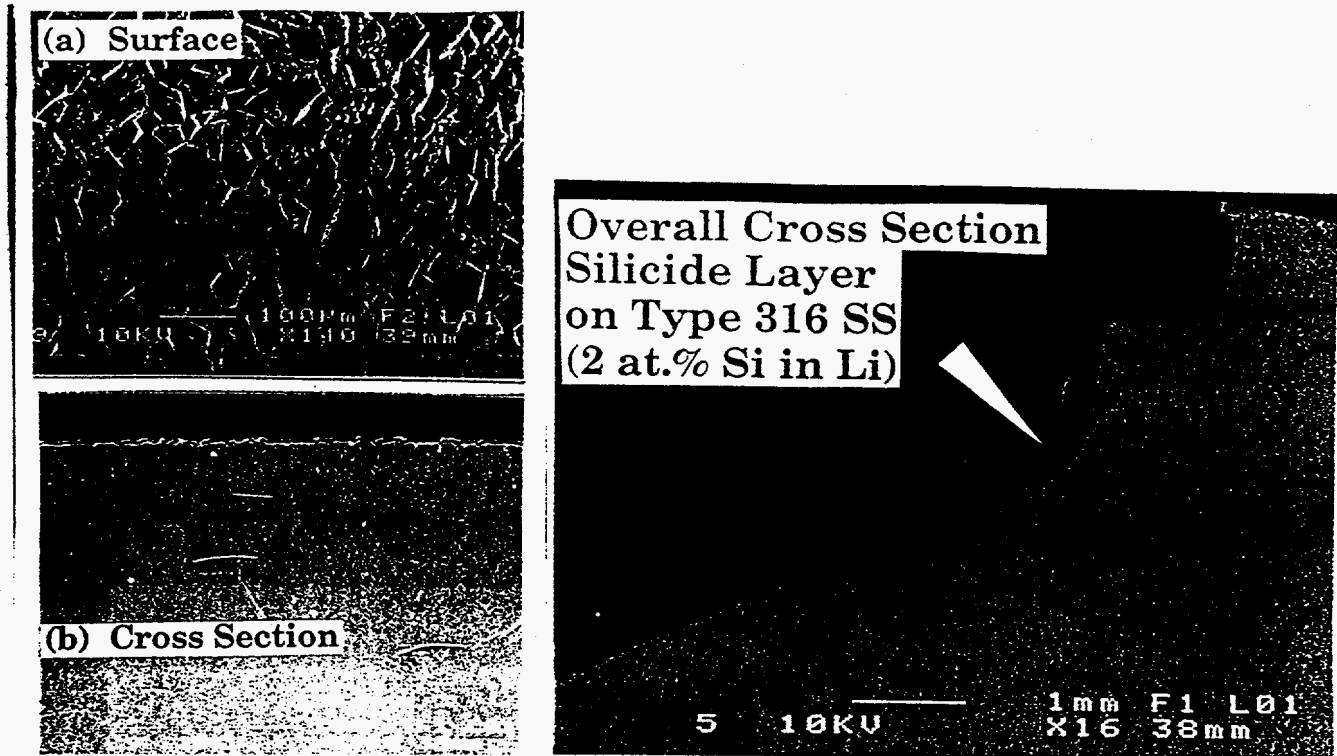


Fig. 8. Silicide coating formed on Type 316 stainless steel in liquid Li at 650°C  
 (a) surface, (b) cross section, and (c) more extended region of (b)

#### 2.4. Oxygen or nitrogen charging of the surface of V-5Cr-5Ti

In the event that metallic solutes dissolved in Li (e.g., Ca, Y<sup>#</sup>, or Mg) do not produce intermetallic phases or diffusion interactions with V or its alloys are very slow, another fabrication approach can be adapted to facilitate formation of an insulating coating. It is well known that O can be incorporated into the interstitial sublattice in body-centered-cubic (bcc) V and its alloys [10]. Thus, if O or N is present in the alloy (as a reactant), these elements may have a higher affinity for solutes, such as Ca or Mg dissolved in Li, compared to that of the alloy elements. In the bcc lattice of V-5Cr-5Ti, O can occupy interstitial sites within a lattice up to several atomic percent. Oxygen charging of V-5Cr-5Ti was conducted at temperatures between 500 and 1030°C in flowing high-purity Ar and N<sub>2</sub> (99.999%) that contained impurity oxygen for times up to 48 h. The weight gain vs. reciprocal temperature is shown in Fig. 9.

<sup>#</sup>Yttrium does not dissolve in liquid Li; nonmetallic impurities (C, H, O, N) reacted with Y. The reaction layer was identified by X-ray diffraction as a YH<sub>2</sub> cubic phase cf. Y (HCP). ICP was used to determine H below 5 at.% and Li below 200 wt. ppm. Therefore, Y-V intermetallic coatings on V were produced by a molten salt technique (ref. [9]).

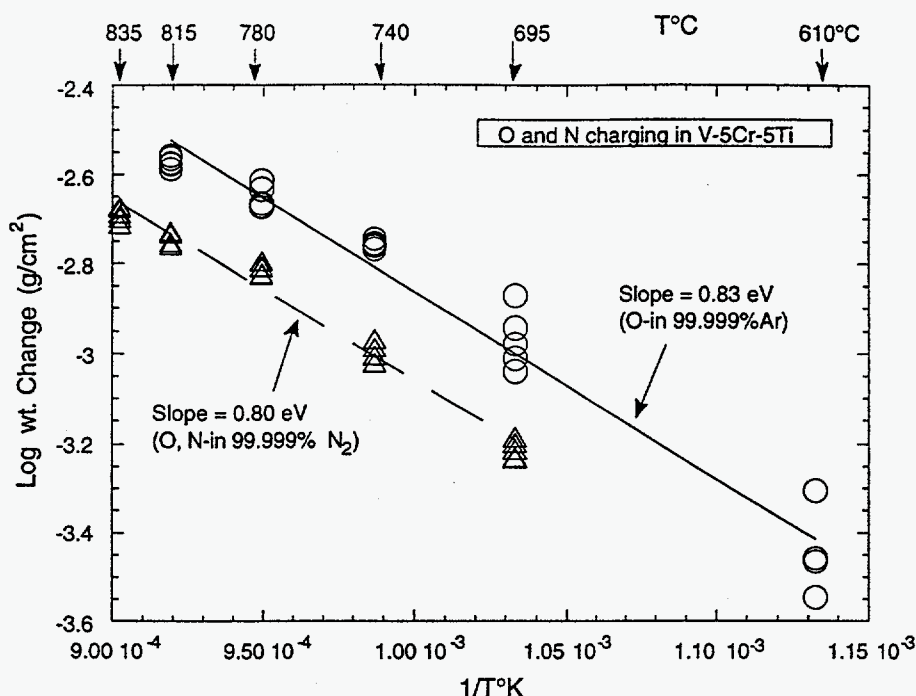


Fig. 9. Weight gain of V-5Cr-5Ti vs. reciprocal temperature after exposure to flowing Ar and N<sub>2</sub> for 48 h

### 3. Formation of ceramic coatings on high-temperature alloys

Ceramic coatings were produced (a) by gas-phase oxidation of intermetallic coatings under controlled conditions (e. g., Al<sub>2</sub>O<sub>3</sub>), (b) reaction of intermetallic layers with dissolved O or N in liquid Li (e.g., TiN), or (c) reaction of dissolved oxygen at the surface of V-5Cr-5Ti (500–10,000 ppm) with a dissolved solutes such as Ca in liquid Li (e.g., CaO).

#### 3.1. Al<sub>2</sub>O<sub>3</sub> coating on stainless steels in air

Al<sub>2</sub>O<sub>3</sub> electrical insulator coatings were produced on intermetallic aluminide layers (FeAl) formed on Types 304 and 316 stainless steel in liquid Li (Fig. 4) by air oxidation at 1000°C. Al<sub>2</sub>O<sub>3</sub> coating layers were shown to be very good insulators at ambient temperatures. Further tests were not conducted in liquid Li because of previous results indicating that Al<sub>2</sub>O<sub>3</sub> was not compatible in liquid Li. [5]

#### 3.2. TiN coating on Ti in liquid-Li

Titanium nitride (TiN) is a well-known ceramic material that exhibits electronic conduction and is thermodynamically stable in liquid Li. TiN films were produced by exposure of Ti to Li that contained N. A sample of pure Ti and a pair of Ti electrodes were

placed in small capsules containing liquid Li and  $\text{Li}_3\text{N}$  for seven days at  $710^\circ\text{C}$  to investigate the formation of TiN. An attempt was made to enhance the resistivity of in-situ-formed TiN films by adding to the Li small amounts of Al, Si, and Mg, which might be incorporated into the films. One sample and set of electrodes was nitrided in Li containing  $\text{Li}_3\text{N}$  and another was immersed in pure Li. The electrical resistance of the films was  $1.0$  to  $1.5 \Omega$  and increased slightly with temperature, which is indicative of metallic conduction. The calculated resistivity ( $r$ ) values of doped TiN range from  $\approx 800$  to  $3900 \Omega\text{-cm}$ .

### 3.3. CaO coating on V-5Cr-5Ti in liquid Li

Several experiments were performed to test the hypothesis proposed in section 2.4. Samples of V-5Cr-5Ti were heat-treated in flowing  $\text{N}_2$  or Ar at temperatures of  $510$  to  $1030^\circ\text{C}$  to charge the surface of the alloy with N or O. Then the samples were immersed in Ca-bearing liquid Li for four days at  $420^\circ\text{C}$  to investigate the formation of CaO. Figure 10 shows an SEM photomicrograph of the surface and cross section of CaO on a V-5Cr-5Ti specimen together with an EDS spectrum from the CaO layer. For specimens exposed to Li containing Ca at  $700^\circ\text{C}$ , a CaO film that contained 12% V formed. The film had of a thick outer layer and a transparent inner layer as shown in Fig. 11.

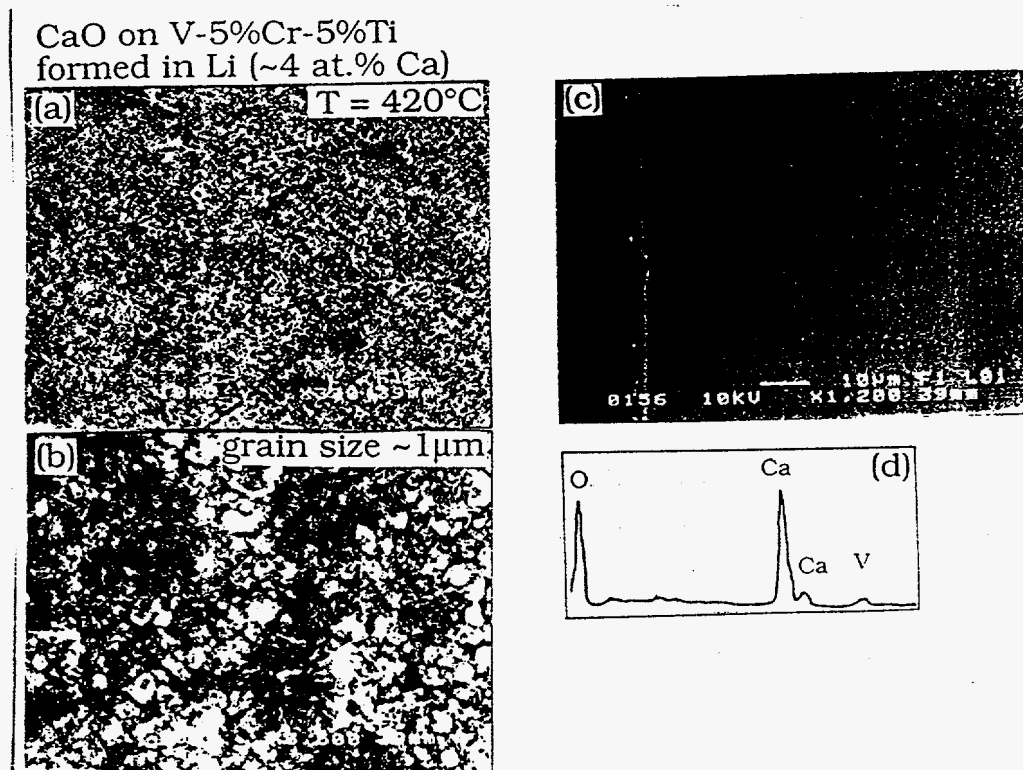


Fig. 10. (a) SEM photomicrograph of surface of CaO layers on V-5Cr-5Ti, (b) enlargement of part of (a), (c) cross-sectional view, and (d) EDS spectrum from CaO layer formed  $416^\circ\text{C}$

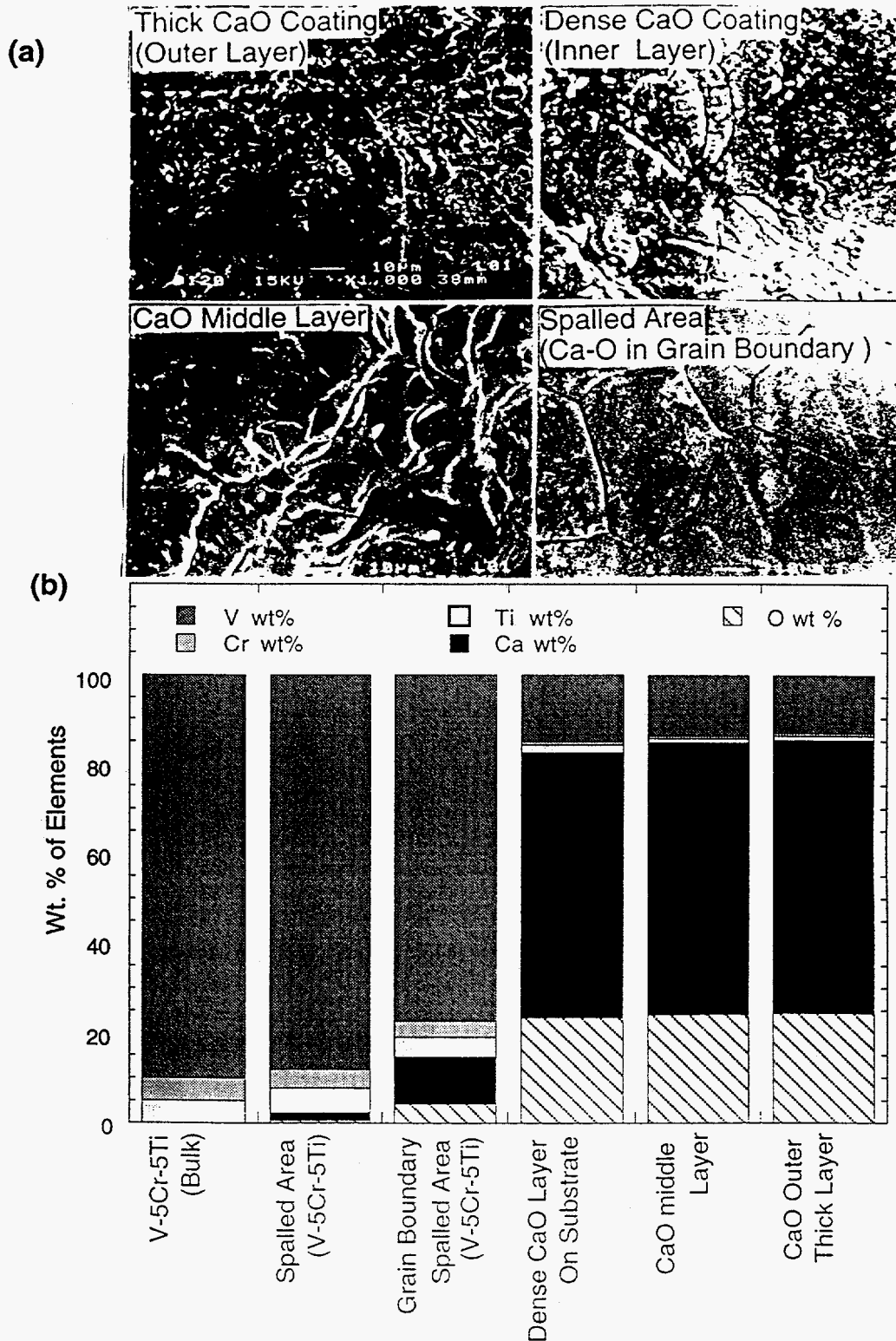


Fig. 11. (a) SEM micrograph of surface of CaO layers on oxygen-charged V-5Cr-5Ti: CaO layer formed at 698°C and (b) composition of CaO layer obtained from EDS analysis.

V-5Cr-5Ti has smaller coefficient of thermal expansion than that of stainless steel ( $9.2 \times 10^{-6}/K$  vs.  $17 \times 10^{-6}/K$ ), as shown in Fig. 12. The value for the V-5Cr-5Ti is relatively close to that of most of the ceramic insulator materials. Consequently, less stress will develop between a V-alloy and a ceramic insulator during thermal cycling conditions. [3] However, a CaO insulator formed in-situ on a V-alloy will be subjected to a compressive stress during cooling.

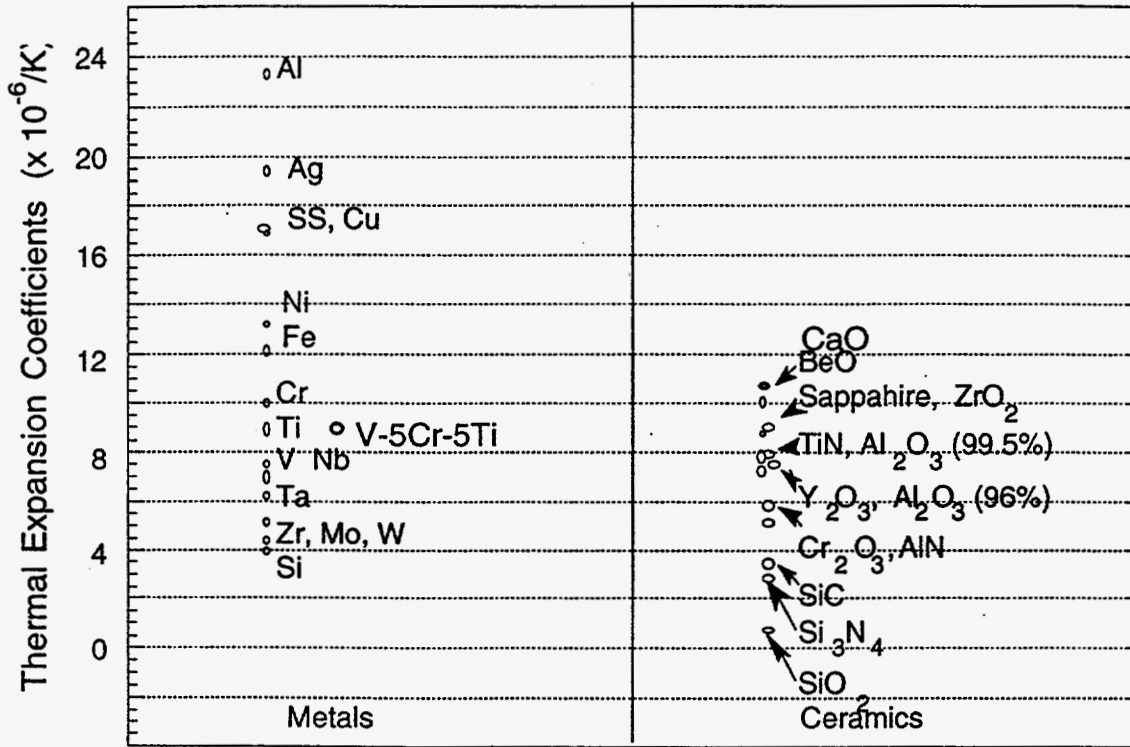


Fig. 12. Thermal expansion coefficients for various metals and ceramics

Temperature dependent electrical resistance showed predominantly ceramic insulator behavior (Fig. 13). When direct current was supplied through the electrodes at  $539^\circ C$ , polarization behavior was observed and the ohmic values increased as shown in Fig. 13.

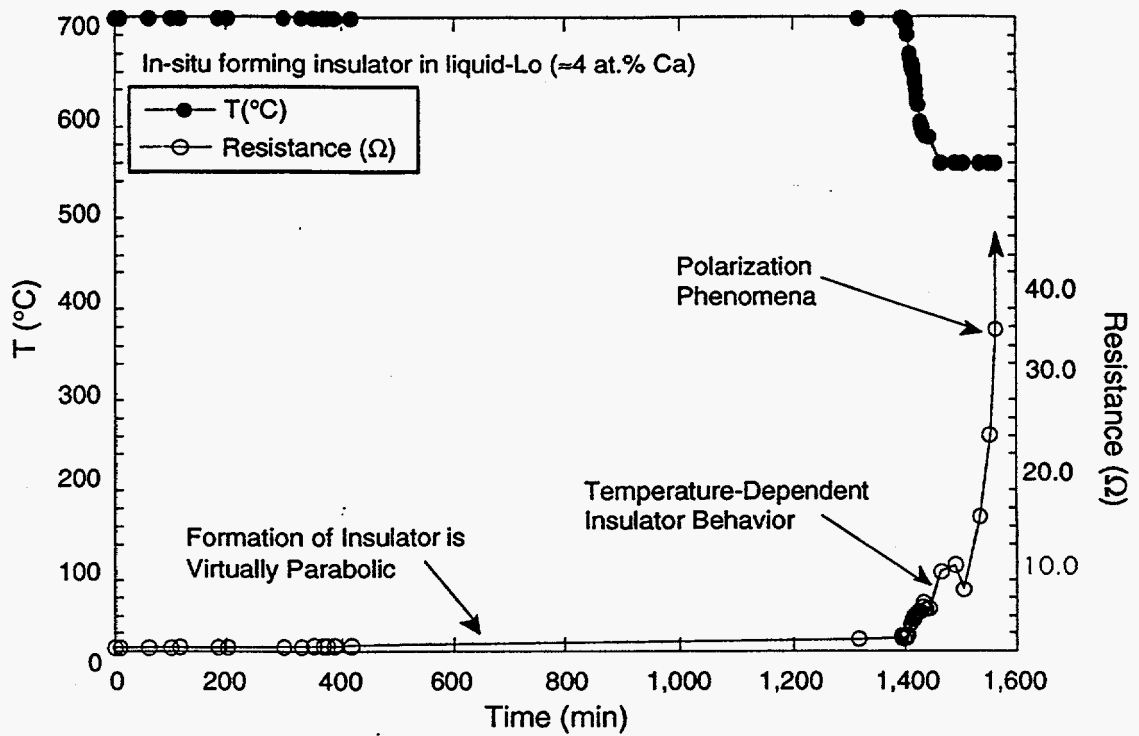


Fig. 13. Temperature and in-situ electrical resistance of CaO coating in liquid Li containing 4 at.% Ca as a function of time

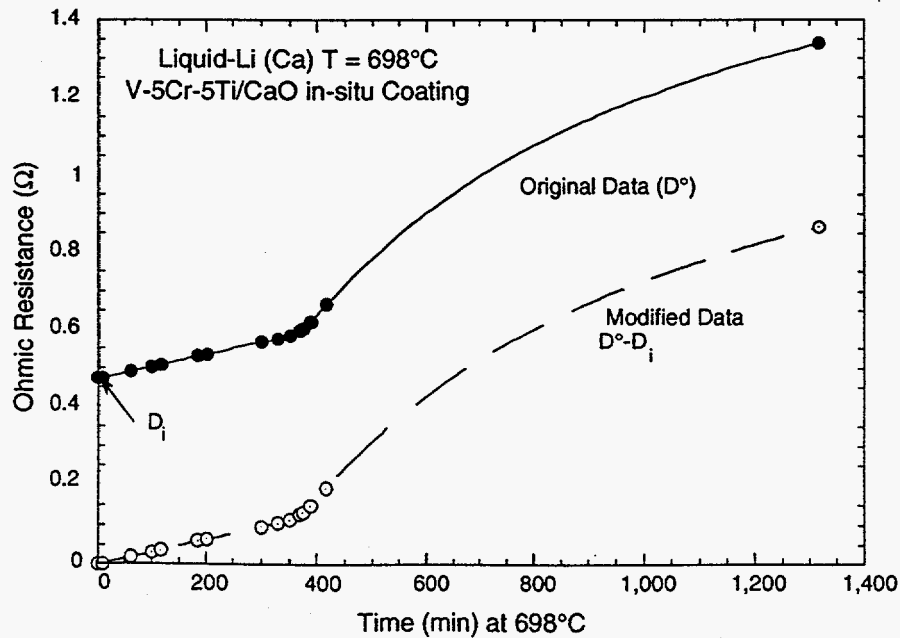


Fig. 14. In-situ electrical resistance of CaO coating in liquid Li containing 4 at.% Ca versus time: details of Fig. 13

#### 4. Determination of Ca-Li phase diagram

Before and after tests in which V-alloy samples were coated, the composition of liquid Li was determined by heating and cooling curves where temperature was monitored as a function of time. Several Ca compositions of the Li were used to form CaO coatings on oxygen-charged V-5Cr-5Ti specimens. Figure 15 shows the Li-rich portion of Ca-Li phase diagram determined in this study.

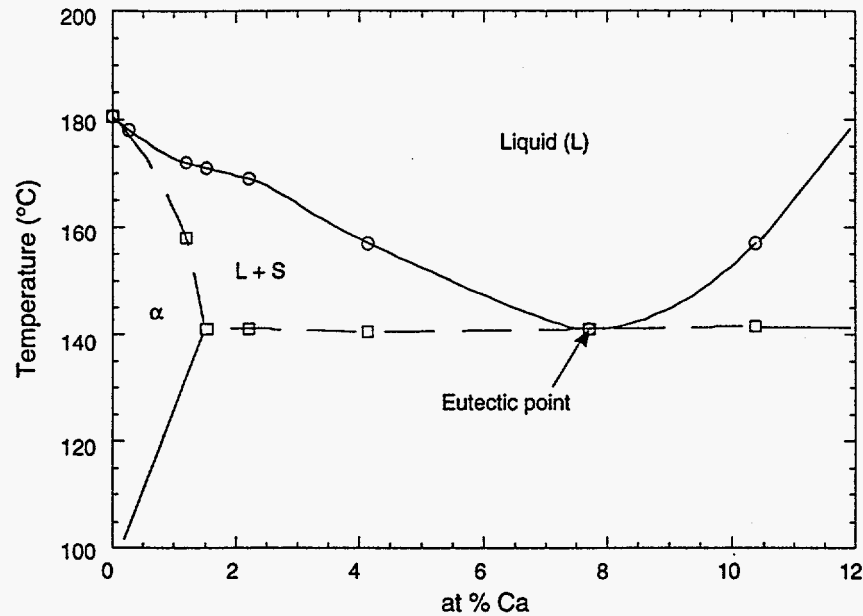


Fig. 15. Li-rich region of the Ca-Li phase diagram

#### 5. Conclusions

Based on liquid Li compatibility tests of coatings produced on V-base alloys, a fabrication method was developed for in-situ insulator coatings in a liquid-Li environment. Surface modification via high-temperature liquid-phase deposition can provide intermetallic phases on V-base alloys. This process is facilitated in liquid Li because surface contamination by O or oxide films is virtually eliminated, and the process to produce homogeneous coatings on various surface shapes can be controlled by exposure time, temperature, and composition of the liquid metal. Conversion of intermetallic or O and N enriched layers to an electrically insulating coating (e.g., AlN for intermetallic aluminide coatings and CaO for surface O-enriched V-5%Cr-5%Ti) in liquid Li was demonstrated in the temperature range of 416 to 880°C. A CaO layer formed relatively easily in liquid Li containing Ca at 416°C. Additional work will be performed to improve the mechanical stability of the coatings during thermal cycling and to establish the mechanisms for self-healing of the coatings.

## Acknowledgments

The author appreciates interactions with Drs. D. L. Smith, R. Mattas, and C. Reed regarding the applicability of the work to fusion reactor designs and with Dr. T. F. Kassner for the fruitful discussions and guidance in liquid-Li-related experimental work. B. Tani of the Argonne Analytical Chemistry Laboratory provided the X-ray diffraction studies. G. Dragel and R. W. Clark assisted the liquid Li experimental work.

## References

1. C. C. Baker et al., *Tokamak Power System Studies FY 1985*, Argonne National Laboratory Report ANL/FPP-85-2 (December 1985).
2. Y. Y. Liu and D. L. Smith, *Ceramic Electrical Insulators for Liquid Metal Blankets*, *J. Nucl. Mater.*, **141-143**, 38 (1986).
3. T. Kammash, *Fusion Reactor Physics*, Chapter 15, Ann Arbor Science Pub. Inc., Ann Arbor, MI (1975), pp. 405-439.
4. R. F. Mattas, B. A. Loomis, and D. L. Smith, *Vanadium Alloys for Fusion Reactor Applications*, *JOM*, **44**(8), 26 (1992).
5. J.-H. Park, T. Domenico, G. Dragel, and R. W. Clark, *Development of Electrical Insulator Coatings for Fusion Power Applications*, Proc. 3rd Int. Symp. on Fusion Nuclear Technology (ISNFT), June 27-July 1, 1994, Los Angeles, CA.
6. R. J. Lauf and J. H. DeVan, *Evaluation of Ceramic Insulator for Lithium Electrochemical Reduction Cells*, *J. Electrochem. Soc.*, **139**, 2087-2091 (1992)
7. M. Hansen, *Constitution of Binary Alloys*, McGraw-Hill, New York (1958).
8. F. A. Shunk, *Constitution of Binary Alloys, Second Supplement*, McGraw-Hill, New York (1969).
9. M. R. Fox and J.-H. Park, *Electrical Insulator Coatings for Liquid-Metal Blanket Applications- Yttria Coating on Vanadium Fusion Reactor Materials Semiannual Progress Report for the Period Ending September 30, 1992*, DOE/ER-0313/13 (1992).
10. A. U. Seybolt and H. T. Sumsion, *Vanadium-Oxygen Solid Solutions*, *J. Metals Trans. AIME*, **292-299** (1953).